Journal of Nuclear Materials 463 (2015) 11–21

Contents lists available at ScienceDirect

Journal of Nuclear Materials

journal homepage: www.elsevier.com/locate/jnucmat

Plasma-surface interaction in the Be/W environment: Conclusions drawn from the JET-ILW for ITER

S. Brezinsek [a,b,*,1], JET-EFDA contributors [2]

[a] JET-EFDA, Culham Science Centre, OX14 3DB, Abingdon, UK
[b] Forschungszentrum Jülich, Institut für Energie- und Klimaforschung - Plasmaphysik, 52425 Jülich, Germany

ARTICLE INFO

Article history:
Available online 23 December 2014

ABSTRACT

The JET ITER-Like Wall experiment (JET-ILW) provides an ideal test bed to investigate plasma-surface interaction (PSI) and plasma operation with the ITER plasma-facing material selection employing beryllium in the main chamber and tungsten in the divertor. The main PSI processes: material erosion and migration, (b) fuel recycling and retention, (c) impurity concentration and radiation have be1en studied and compared between JET-C and JET-ILW. The current physics understanding of these key processes in the JET-ILW revealed that both interpretation of previously obtained carbon results (JET-C) and predictions to ITER need to be revisited. The impact of the first-wall material on the plasma was underestimated.

Main observations are: (a) low primary erosion source in H-mode plasmas and reduction of the material migration from the main chamber to the divertor (*factor* 7) as well as within the divertor from plasma-facing to remote areas (*factor* $30-50$). The energetic threshold for beryllium sputtering minimises the primary erosion source and inhibits multi-step re-erosion in the divertor. The physical sputtering yield of tungsten is low as 10^{-5} and determined by beryllium ions. (b) Reduction of the long-term fuel retention (*factor* $10-20$) in JET-ILW with respect to JET-C. The remaining retention is caused by implantation and co-deposition with beryllium and residual impurities. Outgassing has gained importance and impacts on the recycling properties of beryllium and tungsten. (c) The low effective plasma charge ($Z_{eff} = 1.2$) and low radiation capability of beryllium reveal the bare deuterium plasma physics. Moderate nitrogen seeding, reaching $Z_{eff} = 1.6$, restores in particular the confinement and the L-H threshold behaviour. ITER-compatible divertor conditions with stable semi-detachment were obtained owing to a higher density limit with ILW. Overall JET demonstrated successful plasma operation in the Be/W material combination and confirms its advantageous PSI behaviour and gives strong support to the ITER material selection.

1. Introduction

A coherent approach of good plasma performance with full first-wall compatibility is required to ensure safe and reliable plasma performance in future fusion devices such as ITER [1]. The use of Plasma-Facing Components *(PFCs)* made of carbon-based materials with their good power-handling capabilities decoupled to a certain extent the plasma-scenario development – with good confinement and intrinsic carbon radiation in the divertor [2] – from critical Plasma-Surface Interaction *(PSI)* processes related to lifetime and safety aspects. But unacceptable high steady-state first-wall erosion [3] and unfavourable co-deposition of fuel [4] – causing high tritium retention and a non-sustainable tritium cycle in ITER and beyond – revealed the limitations in the usage of carbon-based PFCs and the need to operate with the only currently available alternative – metallic PFCs. Metallic PFCs were already in use prior to the carbon era, but suffered in tokamaks with limiter configuration and high oxygen content in the plasma from strong high-Z sources, poor screening, and accumulation [5]. The introduction of the divertor in combination with the development of wall-conditioning techniques lead to a renaissance of metallic PFCs. Experience has been gained in CMOD, equipped with molybednum PFCs [6], and ASDEX Upgrade, equipped with a full tungsten first wall [7]. TEXTOR with tungsten limiter PFCs [8] contributed with dedicated experiments to pursue and explore plasma operation at and above the operational limitations. Up to the start of the JET ITER-Like Wall experiment (JET-ILW), no tokamak experience existed in the wall combination proposed for ITER.

* Corresponding author at: Forschungszentrum Jülich, Institut für Energie- und Klimaforschung - Plasmaphysik, 52425 Jülich, Germany.
E-mail addresses: sebastijan.brezinsek@jet.efda.org, s.brezinsek@fz-juelich.de
[1] Presenting author.
[2] See annex of F. Romanelli et al., Fusion Energy 2012 (Proc. 24th Int. Conf. San Diego, 2012) IAEA, (2012).

http://dx.doi.org/10.1016/j.jnucmat.2014.12.007
0022-3115/

ITER employs a full metallic wall consisting of beryllium in the main chamber and, as recently decided, full tungsten divertor from the first day of operation [9]. On the one hand beryllium is selected as low Z-material, tolerable from the point of view of impurity concentration, with excellent potential to getter oxygen in the absence of chemical reactivity with hydrogen. Though beryllium forms layers which are capable to co-deposit fuel, PISCES-B experiments demonstrated lower fuel content in these layers [10] in comparison to carbon. This lower long-term fuel retention in beryllium leads ultimately to the ITER predictions [4], forecasting a significant increase of plasma-operation time without active fuel-removal requirement before the fuel-inventory limit is reached. On the other hand tungsten has been selected owing to the good power-handling capabilities with an extreme high melting point, the low physical sputtering yield, and the low fuel retention. However, in ITER and a reactor, low tungsten concentrations in the order of 10^{-5} are required [11] to avoid excessive core radiation which relies on high tungsten divertor retention and high-density divertor operation. The material choice represents the best currently available compromise to demonstrate fusion power with metallic walls.

The JET tokamak has been transformed from an all-carbon device to a metallic device with the described ITER-like wall combination [12,22]. The JET-ILW provides a unique opportunity to document both the changes from an all-carbon to a Be/W device after PFC replacement and to characterise plasma operation, plasma-edge physics and plasma-wall interaction in the ITER-relevant material mix [13,14]. The JET-ILW is with this respect a test-bed and demonstrated low long-term fuel retention [15] and fully plasma-facing material compatible plasma scenarios [16] in the absence of carbon as intrinsic radiator [17]. A vessel intervention concluded the first year of operation in order to retrieve a selection of PFCs for post-mortem analysis [18]. Plasma operation resumed with emphasis on dedicated tungsten melting studies to give timely input to the first divertor decision in ITER [19], and on confinement studies with the aim to recover the loss in plasma performance [20] in particular with nitrogen seeding [21].

Here, the different experimental findings made with JET-ILW are reviewed and connected to the main PSI processes in the tokamak environment: (a) material erosion and migration, (b) fuel recycling and retention, (c) impurity concentration and radiation. The current physics understanding of these key processes in the JET-ILW revealed that both interpretation of previously obtained JET-C results and predictions to ITER need to be revisited. The impact of first wall materials on the plasma performance was underestimated. This review is structured as follows: Section 2 describes briefly the PFC installation, power-handling qualification, and deals with the residual carbon and oxygen content in the plasma after start of operation. Section 3 is addressing the sputtering processes of beryllium in the main chamber and tungsten in the divertor as well as the associated material migration. The impact of the metallic wall on the global long-term fuel retention, recycling, and outgassing is presented in Section 4. Section 5 reveals the differences in the radiation pattern and plasma purity between JET-ILW and JET-C as well as introduces the beneficial impact of impurity seeding with nitrogen on the confinement. A summary of the physics processes driving the plasma-surface interaction in the Be/W mix and their impact on ITER is given in Section 6.

2. JET-ILW installation, conditioning and first plasma

In JET all PFCs made of carbon-fibre composites (CFC) had been replaced by metallic components in a single shutdown of 18 months duration by the remote-handling system [22]. 15,828 PFCs made of beryllium for the first-wall cladding and limiter as well as tungsten for the divertor and protection tiles in the main chamber were installed, resulting in sum to 2 tons of beryllium in form of bulk Be or Be-coated inconel tiles and 2 tons of tungsten as bulk W or W-coated CFC tiles. The choice between bulk material or coating depends on the requirements concerning erosion/lifetime and power loads. The total amount of installed PFCs and the required installation sequencing underlines the logistic challenge of the project and serves as example for ITER. Fig. 1 shows a comparison of JET-C with JET-ILW: on the left-hand side the previously installed all-carbon wall before extraction of PFCs and on the right-hand side the ILW after the first year of operation. The absence of a distinctive deposition pattern with ILW is striking and indicates drastic changes in material migration.

Despite the same choice of materials, the absence of active cooling forces limitations on the power handling and a much more cautious operation in JET in comparison with ITER equipped with actively cooled PFCs. JET relies purely on inertial cooling, this requires on the one hand maximisation of the power-handling capabilities of the components by design optimisation [23] and on the other hand strict limits on power loads to avoid melting [24]. Dedicated experiments were performed to verify the design of both main PFCs, bulk Be limiters and bulk W divertor, as well as – in view of similar ITER applications – to verify the tools and procedures themselves [25]. The operation in ohmic inner-wall limited discharges and a nominal power load of $P_{in} = 1$ MW m^{-2} at the contact point revealed two power-decay lengths on the limiter surface with an unexpected narrow feature at the apex. This experimental finding has been included in a cross-machine comparison of power-decay lengths, resulting in a scaling law used to predict the power-decay length in ITER [26] and to verify the ITER main chamber PFC design. The narrow power-decay length in connection with a minor toroidal misalignment ($\simeq 1$ mm) of half of the ten protruding inner wall limiters led in auxiliary heated limiter discharges ($JPN83620, I_P = 1.7$ MA,$B_t = 2.3$ T,$P_{NBI} = 5$ MW for 8 s) to peak power loads of $P_{in} = 6$ MW m^{-2} and beryllium melting. However, this slight damage did not prevail further operation in limiter configuration, but demonstrated that the assumption of symmetric toroidal power distribution is critical [25].

Though the PFC exchange was carried out in one shutdown – in contrast to ASDEX-Upgrade with the sequential PFC replacement over several years [7] – both experiments share common, crucial questions with respect to the residual carbon content: by how much is the carbon content in the plasma reduced and how much effects the residual carbon the plasma operation and impacts on PSI processes? In JET, no active cleaning of the inconel vessel took place, thus a natural reservoir of carbon was present after pump down and the initial conditioning. The conditioning cycle itself consisted of pumping at a vessel temperature of 473 K, baking at 593 K, and a series of glow discharges in deuterium accumulating 200 h of

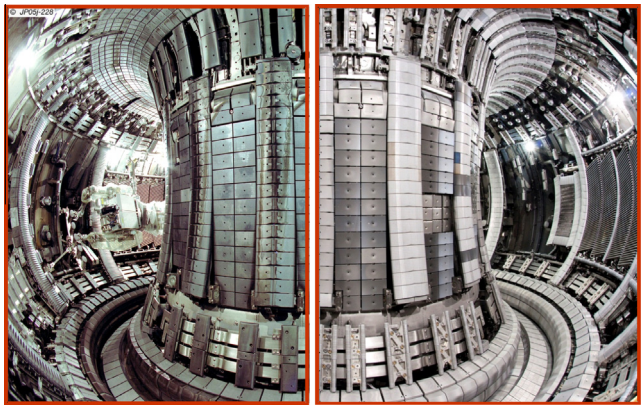

Fig. 1. Transformation of JET: From an all-carbon (JET-C) to an ITER-like device (JET-ILW) with Be main chamber and W divertor.

low temperature plasma and ion bombardment of the freshly installed components [27]. Be-head evaporations were not required in contrast to a conditioning cycle in JET-C. After a major shutdown in JET-C, the first plasmas lasted typically a few hundreds of miliseconds and conditioning by repetitive plasma operation was required to prolong the plasma duration. The behaviour with JET-ILW is with this respect different and allowed an easier plasma access with sustainable breakdown and long lasting plasma in the first attempt which can be attributed to the good oxygen gettering properties of beryllium [13]. All subsequent plasma breakdowns have been, apart from technical set-up failures, successful and no further plasma conditioning was required over the whole initial campaign. This is in strong contrast to JET-C operation where hydrogen-rich carbon co-deposits impacted the plasma breakdown by outgassing [28]; the controlled breakdown with the JET-ILW is in-line with the reduction of radiation by impurities and fuel. In an analogue manner, the averaged carbon and oxygen impurity levels in the plasma-edge layer during the plasma current flat-top phase dropped strongly with ILW in comparison with JET-C. Fig. 2a shows the reduction by more than one order of magnitude of the carbon edge content visualised by *CIII* emission normalised to the edge density. In the initial phase of plasma operation, a short clean-up period in carbon can be identified before almost steady-state conditions set in [17] with a slight increase in the period of high auxiliary power operation at the end of the first year. The carbon content remained low and almost constant in the second campaign executed after the tile intervention confirming an intact metallic first wall. The visual inspection during the intervention corroborated the spectroscopic observations – no significant damage of W-coated PFCs. The JET-ILW represents for the whole collection of studies presented here a valid test bed for a tokamak with beryllium first wall and tungsten divertor as envisaged in ITER.

The initial phase of plasma operation was affected by an air leak (leak rate: 1×10^{-3} mbarls^{-1}), nevertheless, the oxygen edge concentration in JET-ILW plasmas (Fig. 2b) was about one order of magnitude below a typical concentration in JET-C plasmas after vessel opening and substantial exchange of PFCs [27]. Beryllium PFCs in the main chamber which are not directly exposed during the limiter start-up phase to deuterium or beryllium ions are likely oxidised forming thin BeO-layer. The oxygen gettering capability of beryllium saturates in time which might explain that during normal plasma operation, oxygen levels are less pronounced suppressed than carbon levels.

3. Material erosion, transport and deposition

As demonstrated in the previous section, the PFC exchange led to a suppression of residual oxygen and carbon in the plasma

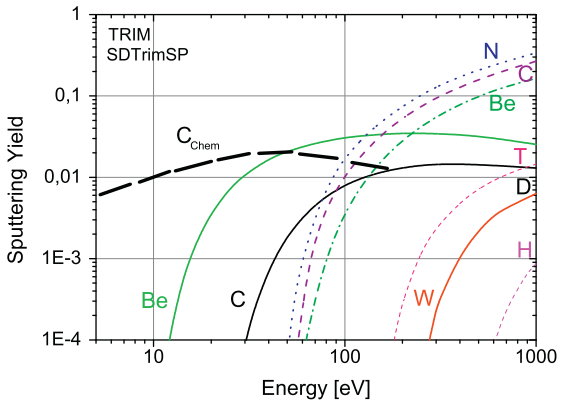

Fig. 3. Predicted physical sputtering yield of *Be, C, W* by *D*, and *W* by *Be, C, N* in binary-collision approximation. The sputtering yield for chemical erosion of carbon by deuterium at lowest impact energies is supplementary added.

leaving beryllium to be the main intrinsic impurity. A key issue is the source strength determination of beryllium in the JET-ILW and the comparison with carbon in JET-C in the absence of chemical erosion of beryllium at low impact energies as predicted by literature. Calculations by TRIM [29] in the binary-collision approximation predict slightly higher physical sputtering yields for beryllium (Fig. 3) at impact energies above the energy threshold which are usually present in limiter conditions for deuterons and charge-exchange neutrals in diverted plasmas. Previous ITER predictions assumed a comparable primary impurity source in an all-C and a Be/W device [4] that had fundamental consequences on material transport, deposition and fuel retention. The determination of the impurity composition is also essential to describe the tungsten source strength in the divertor where physical sputtering of tungsten will not be determined by fuel ions owing to their low mass, but due to plasma impurities. Fig. 3 shows the corresponding predicted physical sputtering yields and impact energy thresholds for tungsten sputtering by C, N, Be which needs to be compared with actual measurements.

In order to interpret the campaign-integrated footprint of erosion and deposition in the JET vessel, it is useful to distinguish between the operational time in limiter configuration with pure Be interaction and divertor configuration with Be/W interaction. The total operational time in the first year of JET-ILW operation (2011–2012) amounts 19 h of which 12 h were executed in divertor configuration. This needs to be compared with the last JET-C campaign (2008–2009) and 33 h total operational time of which 12 h were in limiter configuration. The separation allows to distinguish between material migration paths in these two configura-

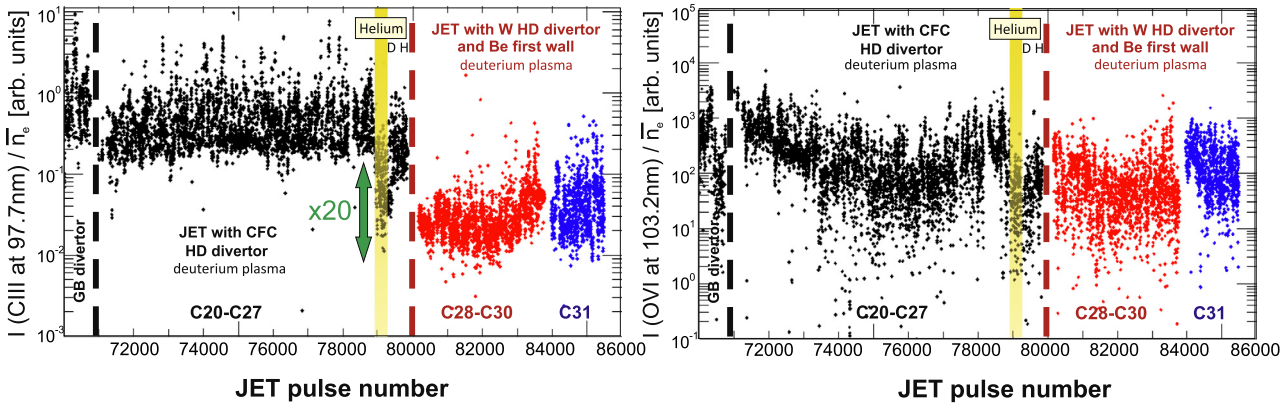

Fig. 2. From JET-C to JET ILW: C ($CIII/n_e$) and O edge plasma content (OVI/n_e) during the divertor phase as function of discharge number.

tions. Note that in contrast to ITER, where long-pulse operation under steady-state conditions for several hundred seconds is foreseen, the plasma duration in JET-ILW is limited to tens of seconds with a factor 5 larger ratio of limiter-to-divertor time.

3.1. Beryllium erosion and migration in limiter plasmas

Dedicated discharges in limiter configuration were performed to assess the erosion of the beryllium first wall. The local plasma conditions at the inboard limiters and within the deuteron impact energies varied in the range of E_{in} = 35–200 eV under an impact angle of about 60°. The effective Be sputtering yield $Y_{Be}^{tot} = \frac{\Gamma_{Be}}{\Gamma_D}$ at the limiter contact point was in-situ determined by optical emission spectroscopy observing *BeII* (527 nm), representative for Be^+ resulting from beryllium erosion, and D_β, representative for the recycling flux or impinging deuteron flux under ionising conditions. In Fig. 4a is this gross erosion yield depicted as function of the local electron temperature (T_e) averaged over the observation spot. Y_{Be}^{tot} increases with T_e from 4% to more than 100% due to beryllium self-sputtering at the highest T_e or impact energies E_{in} [30]. The beryllium sputtering measurements in JET are currently applied to benchmark the Monte-Carlo code ERO taking into account the local geometry, the impact angles, impact energies and two sets of Be sputtering yields obtained from MD calculations, TRIM calculations and laboratory experiments [31]. Current modelling results (Fig. 4a) show an overestimation of the effective sputtering yield by a factor two for the best match between experiment and modelling. ERO has been previously applied to predict the lifetime of ITER first wall modules [32] which would be prolonged by the same factor two assuming the beryllium sputtering data applied in ERO is responsible for the discrepancy.

The measured Y_{Be}^{tot} is at high impact energies about a factor two larger than the corresponding Y_C^{tot} in JET-C; the impact of self-sputtering at these energies is still minor with carbon. In contrast, at the accessible lowest impact energies in limiter discharges Y_{Be}^{tot} is lower than the corresponding Y_C^{tot} in JET-C. However, though no temperature assisted chemical erosion exists with beryllium, chemical assisted physical sputtering (CAPS) of Be via BeD has been identified by optical spectroscopy and contributes additionally to Y_{Be}^{tot}. At an impact energy of e.g. E_{in} = 75 eV CAPS contributes to about 1/3 of the effective beryllium sputtering yield which needs therefore be written as $Y_{Be}^{tot} = Y_{Be}^{phys} + Y_{Be}^{chem}$ [30]. The appearance of Y_{Be}^{chem} is likely caused by the supersaturation of the beryllium surface by the impinging deuteron flux density, which induces a transient deuterium surface coverage of more than 50%, leading to both (a) the appearance of CAPS as additional channel with the release of BeD_x with $x = 1 \ldots 3$ and (b) at higher concentrations potentially to dilution of beryllium at the surface and reduction of Y_{Be}^{tot}. Indeed Fig. 4b reveals the dependence of Y_{Be}^{tot} on the surface temperature in a series of identical limiter discharges with gradual increase of the tile temperature until equilibrium between heat-up during plasma exposure and cool-down between discharges occurred. The value at highest surface temperatures represents the surface-temperature independent bare Y_{Be}^{phys} without any measured CAPS as well as low deuterium content in the interaction layer due to outgassing. Further details about CAPS in the JET-ILW, MD modelling, and PISCES-B are described in [30,33,34]. However, it needs to be stressed that both, physical and chemical assisted physical sputtering, have an energetic threshold that inhibits erosion at lowest impact energies. This is in contrast to chemical erosion of carbon and carbon layers which can also be eroded by low energetic neutrals at room temperature.

A gross erosion yield of 10% is representative for the campaign-averaged beryllium erosion in limiter configuration in the first JET-ILW campaign. This translates to a gross erosion rate of 4.1×10^{18} Be/s or an integral of 1.5 g Be sputtered from one centred inner-limiter tile ($A_{tile} = 0.025 m^2$) in the view of the spectroscopic system (A_{spot} = 0.011 m^2). This can be compared with a net erosion of 0.8 g Be deduced from post-mortem tile profiling for a comparable beryllium tile or a net erosion rate of 2.3×10^{18} Be/s considering the total exposure time in limiter configuration during the campaign [18]. The comparison of spectroscopy and post-mortem analysis reveals a factor two between gross and net beryllium erosion with JET-ILW. The net carbon erosion rate of a corresponding tile in JET-C is twice as high as the net beryllium erosion rate in JET-ILW, however, taking into consideration the different number of interacting limiters in JET-C (#16) and JET-ILW (#10), the discrepancy of the primary impurity source in limiter configuration reduces to 25%. For the complete beryllium source estimation both, spectroscopy and post-mortem analysis, must extrapolate the local information to the total limiter-interaction area which represents a fraction of the total inner wall protruding limiters (A_{lim} = 4.5 m^2), but have less interaction area due to shadowing effects [35]. The main fraction of beryllium eroded at the limiters stays within the main chamber, deposited in recessed areas like the limiter wings, and only a small fraction of eroded beryllium neutrals escapes geometrically from the main chamber into the divertor. Indeed the initial experiment in diverted configuration identified only moderate tungsten surface

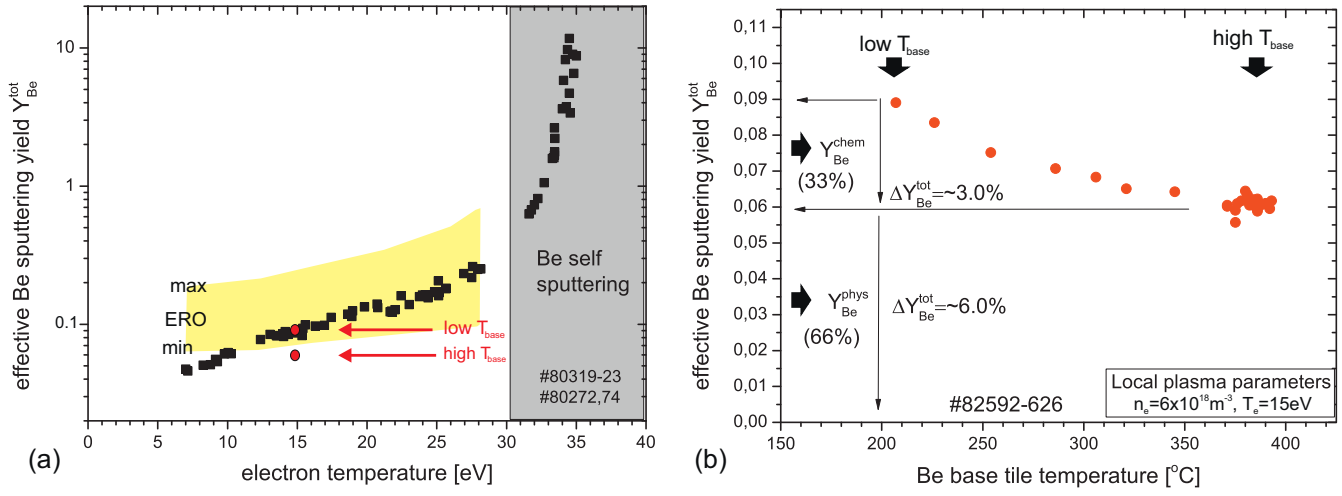

Fig. 4. (a) The effective Be sputtering yield as function of T_e measured in JET-ILW and associated ERO modelling. (b) Composition of the effective Be sputtering yield at E_{in} = 75 eV as function of the Be tile temperature [30].

coverage by beryllium after about 625 s in limiter configuration with dominant beryllium self-sputtering [36]. However, the amount of beryllium entering the divertor in limiter configuration is insignificant in comparison with the amount in divertor configuration.

3.2. Beryllium erosion and migration in diverted plasmas

The present understanding on material migration is predominantly based on tokamaks with carbon-based PFCs and information obtained from optical spectroscopy during plasmas and post-mortem analysis after PFC extraction. The main chamber is identified as primary erosion source and material is transported via scrape-off layer (SOL) flows in normal magnetic field configuration mainly towards the inner divertor where finite deposition occurs [37]. In a subsequent multi-step process, material transport to remote and inaccessible areas takes place, leading to co-deposition and high fuel retention. The later ultimately led to the abandoning of carbon PFCs in ITER due to safety aspects [4]. Despite being a net source, the outer divertor plays only a minor role in the overall migration.

In the JET-ILW, no main chamber plasma-facing material (beryllium) is installed in the divertor, thus, all Be ions flowing into the tungsten divertor are originated from the main chamber during diverted plasma operation. Homogenous Be and BeD light emission in toroidal and poloidal direction at the inner wall can be measured by spectroscopy in divertor configuration resulting from erosion processes in these recessed areas in the SOL. The origin of these processes is twofold: (i) energetic charge exchange neutrals (CXN) are impinging the recessed inner-wall area ($A_{wall} = 18.5\ m^2$) equipped primarily with cladding tiles ($A_{clad} = 11.2\ m^2$) of which 2/3 are made of Be-coated inconel and 1/3 of tungsten tiles located between adjacent poloidal limiters and positioned typically 6–10 cm behind the separatrix. (ii) Residual plasma flux is reaching the recessed wall and limiters. The variation of the distance between separatrix and beryllium surface, is causing changes in the Be and BeD particle flux indicating that the residual deuterium ion flux contributes to the beryllium erosion. Though no Be-cladding exists at the outer wall, CXN and residual plasma flux interact with the outer-poloidal limiters and contribute to the Be main chamber source; the degree depends on plasma conditions and distance of the separatrix to these PFCs.

Beryllium material probes installed between cladding tiles show at different locations measurable erosion after the initial JET-ILW campaign [38] confirming that this area is a zone of net erosion. The beryllium source from the inner wall was quantified ex-situ by RBS to 12.2 g in the integrated divertor time. The corresponding erosion rate during divertor operation amounts to 0.78×10^{18} Be $m^{-2}\ s^{-1}$. The rate can be compared with the erosion rate of 3.14×10^{19} C $m^{-2}\ s^{-1}$ in JET-C (2005–2009) where similar long-term carbon samples were installed and analysed [39]. The erosion rates differ by a factor of 4.0 which reflects essentially the strong reduction of the primary erosion source with the JET-ILW. The global source is even stronger reduced by a factor 5.3 when the different total area of CFC cladding in JET-C to Be cladding in JET-ILW is considered. A difference in the erosion processes is required to explain the discrepancy in the primary source as (a) the CXN flux and the residual plasma flux impinging on the first wall are similar in both wall configurations and (b) the bare physical sputtering of beryllium is larger than carbon (Fig. 3). Indeed this discrepancy can only be explained by chemical erosion of carbon at the lowest, even thermal energies of impinging deuterium ions and atoms solely present in JET-C.

The beryllium migration path in the JET-ILW can be described as follows: (i) neutral Be and BeD from physical sputtering and chemical assisted physical sputtering at the recessed wall enter the plasma, (ii) BeD dissociates and neutral Be is ionised and transported by SOL-flows towards the inner divertor (Fig. 5a) where (iii) significant deposition takes place on top of the inner vertical-target plate (Fig. 5b). Post-mortem analysis confirms almost pure, hydrogen-poor beryllium layers with minor oxygen content at this location as shown in Fig. 5c. The integral beryllium source in the main chamber during divertor operation and the amount of beryllium deposited in the inner divertor is comparable according to initial global balance studies [35]. The comparison with corresponding carbon deposition in the JET-C divertor reveals a factor seven reduction in beryllium divertor deposition with JET-ILW induced by the lower main chamber source.

Within the divertor (Fig. 5b), beryllium performs much less re-erosion/deposition cycles than carbon due to the energetic threshold for physical sputtering of beryllium which inhibits the multi-step transport to the divertor floor, and even further, to the remote areas at the pump-duct entrance. Post-mortem analysis [18] demonstrated that the inner vertical target is only partially covered by beryllium and indeed intact bare tungsten surfaces can be detected. This is confirmed by optical spectroscopy and *WI* emission in the plasma throughout the campaign. The measured effective deposition thickness is in the order of 1/5 of the surface roughness of the W-coatings which makes the analysis challenging. In contrast, the balance between erosion and deposition at the inner-target plate of JET-C was moved strongly towards deposition leading up to thick carbon co-deposits with more than a factor 50 times thicker deposition.

Detailed ERO modelling was applied to compare the transport of beryllium in the JET-ILW once entering the inner divertor leg with the transport of carbon in JET-C [40]. Indeed it is only possible

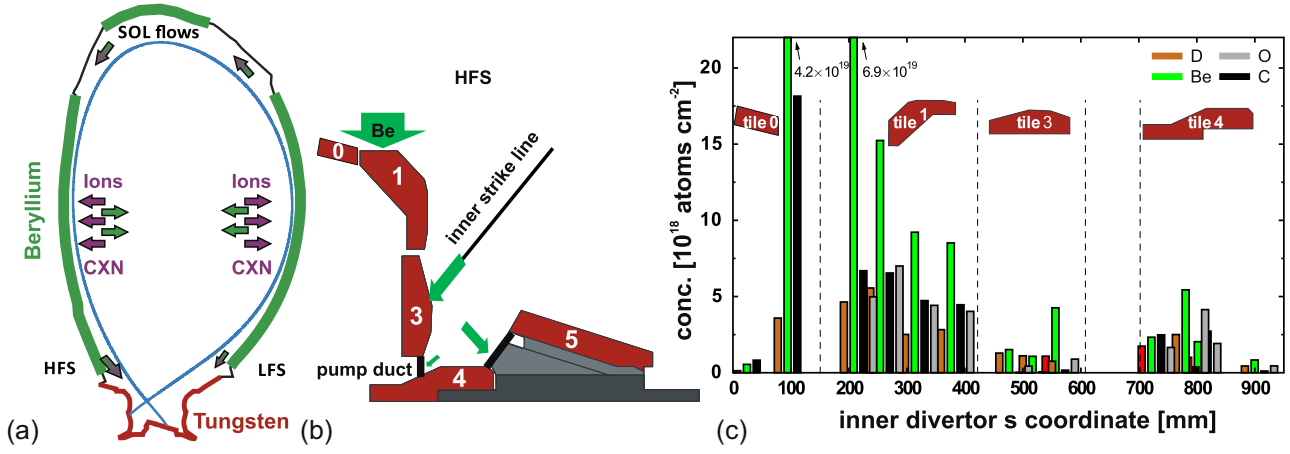

Fig. 5. Global (a) and inner divertor (b) material (beryllium) migration paths with the JET-ILW. (c) Deposition of Be, C, O and D along the inner divertor target plates deduced from post-mortem analysis [42].

to describe the measured beryllium deposition pattern in the inner divertor of the JET-ILW if a factor 5–10 lower initial impurity ion flux (Be^{2+}) in comparison with the carbon flux (C^{4+}) in JET-C is considered which is consistent with spectroscopic observations and the fact that the tungsten divertor plate is not buried by beryllium. This impinging Be ion flux is neutralised at the target, reflected and transported line-of-sight towards the side protection of tile 5. Different deposition monitors [cf. [40] and references within] showed low net deposition with a reduction of about a factor 15 in comparison with JET-C references. The reduction in the material transport towards the inner pump-duct entrance is even more pronounced; a factor 30–50 reduction in deposited material [41] was found. Indeed the thin deposits ($\simeq 1$ μm) on the sloping part of the horizontal-target plate (Fig. 5c) are rich with impurities such as oxygen (from air leaks) and carbon (residual content) [43,44] which reduces effectively the net transport of beryllium by another factor two. This leads to the conclusion that beryllium is only performing line-of-sight transport after physical sputtering processes (about 2 steps) whereas the residual carbon still performs the multi-step transport (about 10 steps) caused mainly by chemical erosion leading to enrichment of carbon in the remote and inaccessible divertor areas. It should be stressed that the overall integral deposition in these remote areas is about two orders of magnitude lower with the JET-ILW than with JET-C. The majority of deposited Be in the divertor remains on top of tile 1 and only a minor fraction is participating in further transport within the divertor.

3.3. Tungsten sputtering and transport in diverted configuration

The tungsten sputtering yield was quantified in-situ by optical emission spectroscopy [45] in L-mode discharges with density ramps reaching partially divertor detachment and impact energies of ions and deuterons around the energetic sputter threshold. Optimised diagnostic access for W spectroscopy is only available at the bulk-tungsten target plate which represents an almost pristine tungsten surface as situated in a net-erosion zone throughout the campaign. It should be noted that this also true for the lower vertical-target plates as post-mortem analysis confirmed, but the spectroscopic view is vignetted and observation of neutral tungsten with penetration depths of a few mm is challenging. The physical sputtering of tungsten is in general determined by impurities and their composition, energy, and flux assuming that the energy overcomes the threshold. Deuterons play only a role at impact energies above $\simeq 250$ eV due to their low mass (Fig. 3).

In JET, the physical sputtering of tungsten can for a wide range of plasma conditions be described by beryllium ion Be^{2+} bombardment with a concentration of about 0.5% with respect to the impinging deuteron flux. Though the fraction of beryllium in the impinging ion flux varies with plasma conditions, the concentration of 0.5% is in very good agreement with the described low primary beryllium source and the beryllium transport into the divertor. Fig. 6a shows the effective sputtering yield as function of T_e at the target plate for comparable experiments in JET-ILW, ASDEX Upgrade and TEXTOR; T_e acts here as proxy for $E_{in} = 3 \times k_B Z_x T_e + 2 \times k_B T_i \simeq 5 \times k_B T_e$ assuming locally $T_e \simeq T_i$. The lines represent TRIM calculations for different impinging species and concentrations as described in Fig. 3. The JET-ILW confirms the expected threshold behaviour for Be^{2+} at low T_e achieved by plasma cooling by deuterium fuelling or impurity seeding. The effective tungsten sputtering yield is above 6×10^{-5} for $T_e > 20$ eV, reflecting fully attached divertor conditions, and more than one order of magnitude below yields determined in ASDEX Upgrade [11] and TEXTOR [46]. In ASDEX Upgrade and TEXTOR, the dominant impurity species is C which has a higher mass and higher charge state than Be and is therefore more effective to sputter W. In ASDEX Upgrade the best fit is achieved assuming an effective impinging impurity species C^{4+} of 1% *to* 2%; C^{4+} includes effectively N, O, and F ions which are present in discharges without boronisation. The lower effective W sputtering yield in JET is a consequence of the low concentration of plasma impurities or, in other words, the high plasma purity owing to the use of Be PFCs as explained in Section 2. The prompt re-deposition of tungsten has been estimated to $\simeq 50\%$ at a magnetic field of 2.5 T by comparing *WI* and *WII*-lines resulting in the deposition of eroded tungsten within one Larmour radius [45] which is in agreement with ASDEX Upgrade [11] and TEXTOR [46]. The divertor retention of tungsten was determined by the comparison of the W concentration in the plasma core and the W source in the divertor and estimated to be about 100 for the open divertor geometry in JET [47].

The operation with inertially cooled PFCs requires mitigation of steady-state power loads to the divertor-target plates in H-mode plasmas with high auxiliary power and energy content. This can be achieved by impurity seeding (N_2) which induces (semi-) detachment at the target plates and mitigates the W sputtering simultaneously as the impact energy of deuterons and impurity ions fall below the physical sputtering threshold as depicted in Fig. 6b. However, Edge Localised Modes (ELMs), filaments which carry energetic deuterons and impurity ions from the hot pedestal region down to target plate, interrupt regularly the quiet (inter-ELM) phase. These particles with energies above the physical sputtering threshold induce tungsten sputtering and can even represent the sole tungsten source as it is shown in Fig. 6b where tungsten sputtering is

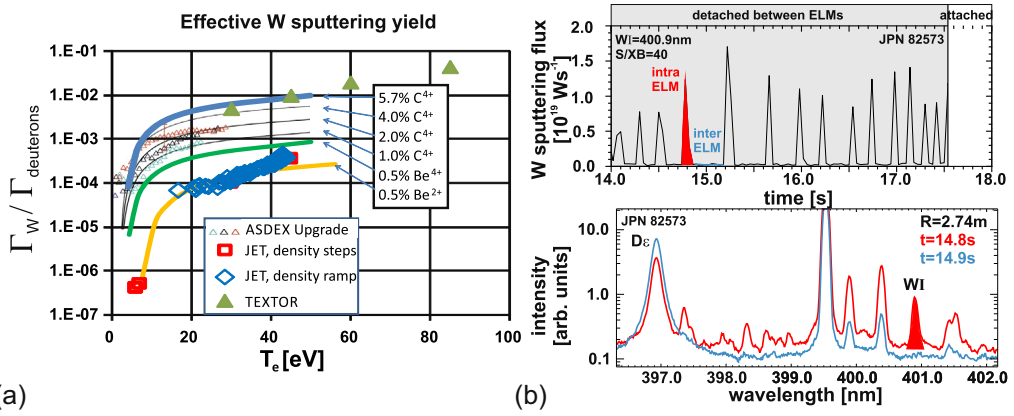

Fig. 6. (a) Physical sputtering yield of W in JET, TEXTOR and ASDEX Upgrade. (b) Top: W sputtering during ELM excursions and detached divertor conditions between ELMs in nitrogen seeded JET-ILW discharges. Bottom: Emission spectrum in the outer divertor covering WI at 400.9 nm recorded in the intra and inter-ELM phase.

fully mitigated in the detached inter-ELM phase. The tungsten source can be distributed in different portions between ELM and inter-ELM phase depending on the electron temperature between ELMs and the ELM frequency. These observations are in agreement with observations made in ASDEX Upgrade [11].

Though ELMs are responsible for at least a fraction of the W production in H-mode plasmas, ELMs are also required to remove W from the confined region by flushing as otherwise W accumulation can occur. A set of W control tools have been developed in JET in order to ensure plasma operation without W accumulation, thus, steadiness over the achievable flat-top phase of more than 10*s*. From the point of view of the source and transport, it is mandatory to keep the inter-ELM source low which requires a minimum deuterium injection rate or significant impurity seeding (to overcome the seeding impurity-induced W sputtering) and sustain a minimum ELM frequency as described in [47]. This restricts the operational window with W in comparison with C divertor in JET-C where no limitations with respect to plasma fuelling existed [16]. H-mode plasmas with sole deuterium fuelling from first wall outgassing – so-called unfuelled plasmas – are in general not stable with the JET-ILW. However, ITER will require semi-detached plasma operation [1] and ELM pacing which will secure both safe operation with respect to the power loads at the target plates as well as will provide quasi-intrinsic W control.

4. Fuel recycling, retention and removal

Implantation and co-deposition of fuel are the main mechanisms for retention in tokamaks. Implantation saturates in principle with impinging ion flux or fluence and co-deposition can increase linearly with ion flux and operational time [4], thus, the dominant mechanism for long-term retention remains the co-deposition of fuel with the main impurity, i.e. Be in JET-ILW as C in JET-C. The change in the fuel content in co-deposits can be, according to fuel-content scalings in Be and C co-deposits deduced in PISCES [10], responsible for about a factor ten of the reduction at the nominal vessel temperature at JET (473 K) assuming otherwise comparable plasmas, i.e. ion flux and impurity concentration, and surface conditions. Co-deposition with tungsten is negligible in comparison with beryllium.

4.1. Long-term retention and fuel removal

Global gas balances, measured as an integral through multiple discharges [48], have been executed in different plasma conditions and confinement regimes in JET-ILW and compared with JET-C reference experiments [49,15]. The long-term retention rate of deuterium normalised to the operational time in diverted configuration phase drops substantially by more than one order of magnitude with introduction of the JET-ILW in all performed experiments to values below 1.5×10^{20} D s^{-1} which represents the absolute upper limit [15]. The drop of a factor 10 to 20, depending in detail on the plasma regime and to a certain extent on the ion flux to the PFCs, is shown in Fig. 7a. The retention rate falls below 1.0×10^{20} D s^{-1} in H-mode plasmas if the 50% longer outgassing period between discharges in JET-ILW in comparison with JET-C is considered, indicating the prominent role of short-term retention. Though the short-term retention, potentially by transient supersaturation of Be and W surfaces, and post-plasma outgassing is in absolute magnitude comparable between JET-ILW and JET-C [50], the relative importance is increased as the underlying long-term retention is dramatically reduced. The outgassing behaviour with a power law of $t^{-0.7}$ had been already observed in JET with toroidal circumferential beryllium belt limiter [51]. The accessible fuel inventory with the JET-ILW was determined in isotope exchange experiments including gas balances with isotope quantification. The exchange by tokamak discharges revealed an inventory of 3×10^{22} D s^{-1} which is ten times lower than in JET-C [52], but during the exchange re-capturing of released fuel in co-deposits in the divertor takes place. Fuel exchange by ion-cyclotron wall conditioning plasmas demonstrated a higher recovery of 5×10^{22} D s^{-1} in absence of co-deposition in the divertor [53] which offers a better perspective as tritium removal techniques in ITER in connection with the accessibility of co-deposits on plasma-facing sides.

The high reproducibility of retention rates deduced in H-mode plasmas in the middle and the end of first year of ILW operation [15] underlines that the dominant mechanism for the residual long-term retention remains unchanged in this period. This points to co-deposition of fuel with Be as dominant process as implantation into the bulk material shall be in principle saturated owing to the large fluence in the main chamber and divertor to the PFCs. But these plasma-specific gas balances can neither provide detailed information on the types of co-deposits nor their exact location. However, supportive spectroscopy suggests that co-deposition by beryllium occurs mainly in the inner divertor and that the contribution of other impurities in these experiments is low which is confirmed by residual-gas analysis and gas chromatography [54]. Post-mortem analysis of PFCs provides complementary information though campaign integrated over all limited and diverted plasmas, resulting in a 15 times lower fuel inventory with JET-ILW in comparison with JET-C [42] and confirming the gas-balance

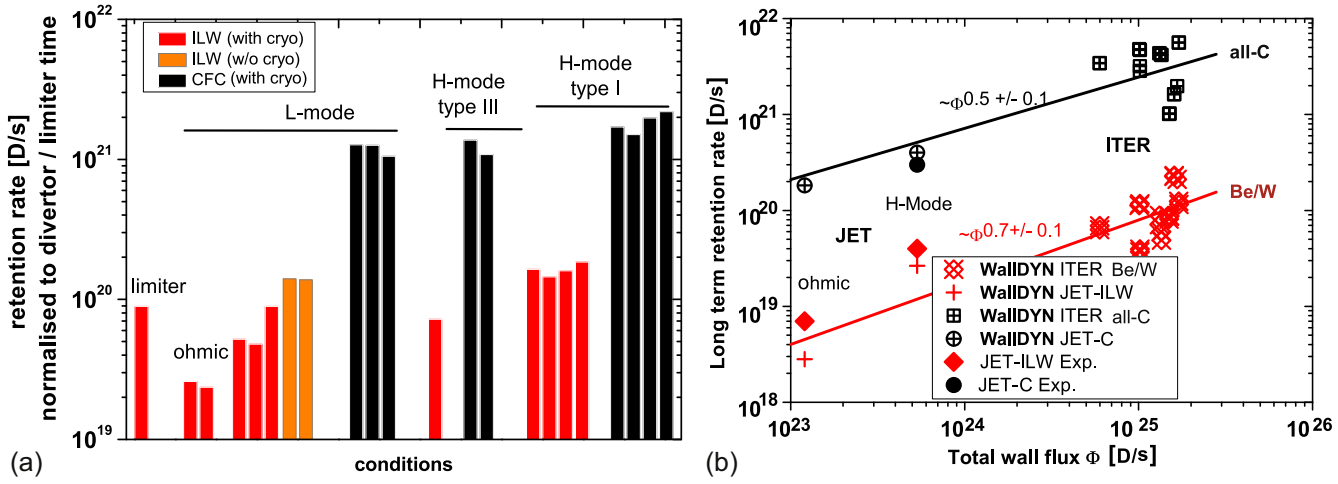

Fig. 7. (a) Long-term fuel retention rates in the JET-ILW measured by global gas balances. (b) Long-term retention rate predictions for ITER made by WallDYN [57] and JET-ILW benchmarks from global gas balances.

measurements. A difference in absolute retention rates exist as the long outgassing phase between the last experiment and the actual tile analysis of about one year impacts strongly on the absolute fuel content in comparison with gas-balance studies and an outgassing period of 1.5 h [30]. The distribution of the fuel can under the assumption of toroidal symmetry be described as follows: one third of the retained fuel is found in the main chamber PFCs (5.7×10^{22} D on the low-field side, 2.8×10^{22} D on the high-field side, 2.1×10^{22} D on the upper wall PFCs) and two third are in the divertor (2.9×10^{23} D in the inner divertor Fig. 5b and 8.6×10^{22} D in the outer divertor) - further details are given in [42]. The retention distribution is largely consistent with the observed migration pattern of beryllium in limiter (Be migration within the main chamber) and divertor operation (Be migration into the divertor) and the corresponding operational time as described before. The observed retention in the limiter phase is consistent with gas-balance measurements (Fig. 7a) in ohmic limiter discharges [15]. The normalisation of the retention to the time in divertor configuration overestimates the retention rate by a about 15% due to the inclusion of the retention which takes place in the limiter start-up phase (3 : 1 ratio between divertor and limiter-configuration duration) [15]. In summary the reduction in the ITER-relevant long-term fuel retention in divertor configuration can be attributed to following processes: (i) The primary impurity source in the main chamber during divertor operation, C in JET-C and Be in JET-ILW, is reduced with JET-ILW leading to less beryllium co-deposition. (ii) Reduced deuterium content in pure beryllium co-deposits in comparison with carbon co-deposits at the JET wall temperatures. The initial prediction was the absolute dominance of the second process, but a fraction of co-deposits are found in divertor areas which have lower surface temperatures than the nominal vessel temperature, and the difference between carbon and beryllium co-deposits shrinks at e.g. 473 K to a factor 5 [55]. Moreover, co-deposition of fuel with beryllium and residual impurities (C,O) occurs in particular on the horizontal-target plates and the fraction of fuel in this mixed layer is higher than in pure beryllium co-deposits [42]. Though the fuel fraction in these layers is high, the overall contribution to the total retention is very low in comparison with the main, pure beryllium deposition area on top of tile 1.

An improved way to predict the tritium retention in ITER is the usage of the WallDYN code [56], verified with JET-ILW gas-balance experiments and applied to predicted ITER plasma backgrounds, instead of simplified experimental scalings of wall fluxes from the same experiments [15]. WallDYN is based on a set of rate equations for a number of pre-defined plasma-surface interaction processes and calculates the global erosion and deposition pattern with the help of a set of discrete interaction points in the poloidal circumference and a redistribution matrix for a given static plasma background. The code provides therefore not only the integral fuel retention, but also the primary impurity sources, the migration path and the final co-deposition areas where the scaling laws for the fuel content are applied [10]. WallDYN has been benchmarked against a set of JET-ILW and JET-C gas balance experiments in ohmic and H-mode conditions [57,15] but adapted to the total outgassing from PFCs according to [50] in order to predict the long-term retention comparable to post-mortem analysis data. WallDYN can reproduce for limiter and divertor plasma conditions qualitatively the observed beryllium migration pattern including the primary erosion sources at the first wall and the deposition of beryllium on top of the upper vertical target in the JET-ILW. In contrast, the co-deposition in the whole carbon divertor, as observed in the JET-C experiments, can be reproduced which essentially confirms the previously described multi-step transport of carbon caused by chemical erosion. This the key difference between JET-C and JET-ILW in modelling and experiment. Fig. 7b shows the good agreement of the deuterium retention rate in the divertor phase as function of the total ion flux to the wall in the experiment and modelling. Extrapolation of the verified code to different ITER background plasmas provides the wide range of long-term fuel-retention rates in ITER which finally results in 3000 to 20,000 full power DT discharges with 400 s duration before the tritium inventory limit is reached [57]. Therefore, the JET-ILW experiment and the WallDYN code confirm the low long-term fuel retention in the Be/W material mix and justified the selection of the ITER-material mix with respect to this safety issue.

4.2. Fuel recycling

The outgassing properties of both beryllium and tungsten PFCs are impacting on the recycling behaviour at the main PFCs. Fig. 8 shows the fuel retention in the limiter phase, plasma contact to the beryllium limiters, and in the divertor phase, plasma contact to the tungsten target plates, for a series of identical discharges in L-mode ($JPN\#81937-81973, I_p = 2.5$ MA, $B_t = 2.4$ T, $P_{aux} = 0.5$ MW) with low fuelling and solely turbo-molecular pumping [15]. Each of the 35 discharges (averaged repetition rate 20 min) remains for about 20 s in the divertor configuration with a typical ion flux to the target plates of 3×10^{22} D s^{-1}. The integral retention drops in the first ten discharges until an equilibrium between short-term retention in the discharges and outgassing during and after the discharge occurs. The inertially cooled tungsten target plates are heated-up by the impinging power load in the first ten discharges until a thermal equilibrium between plasma impact and cool-down phase is reached. Longer breaks between discharges, as indicated in Fig. 8, are causing more outgassing and more retention in the subsequent discharge. As the ion flux to the target plates remains the same in these discharge series, the difference in retention can only be explained by a change of the local recycling connected to the surface temperature increase. The tungsten divertor shows a dynamic behaviour of the deuterium recycling with a recycling coefficient $R < 1$ in these first low fuelled L-mode discharges. Note, that the outer-strike line is located on the pristine bulk-tungsten surface and the inner-strike line on the vertical target which is only partially covered by a thin layer and has intact tungsten areas as discussed in Section 3.

The deuterium recycling is even more dynamic in H-mode plasmas when ELMs are present. An ELM is induced by the crash of the H-mode pedestal and releases hot plasma to the SOL and to the tungsten-target plate. ELMs are conducting on a timescale of 1 ms [58] additional power to the target plate and heat it up in addition to the surface temperature induced by the steady-state heat load reaching 1570 K in regular operation on the bulk-W target plate. Each ELM desorbs deuterium from the tungsten PFCs depending on the actual temperature increase per ELM and its duration. The desorption peaks in the W-coated PFCs are already

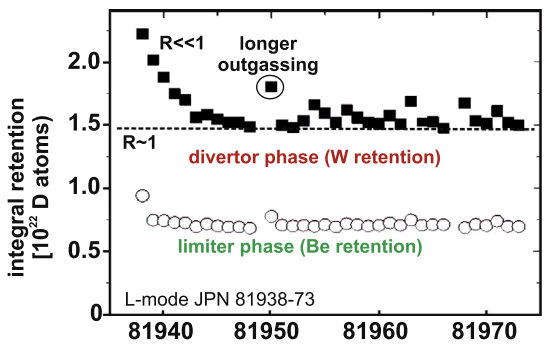

Fig. 8. Active pumping of deuterium by the tungsten divertor in a series of identical JET-ILW L-mode plasmas.

reached at 570 K and 690 K [42] which are exceeded routinely in H-mode due to the inertial cooling. Thus, the accessible deuterium reservoir is partially emptied considering the actual temperature footprint of the ELM on the tungsten target plate. The desorbed deuterium needs to be refilled to reach equilibrium, therefore, the recycling coefficient changes for a short time from $R \simeq 1$ to $R < 1$ after the ELM crash. The deuteron flux to the target plate is used to refill the partially emptied reservoir as externally injected deuterium or deuterium reabsorption cannot provide the required amount in the order of 10^{20} D within a few ms which a typical ion flux of $\sim 10^{23}$ D s^{-1} m^{-2} to the target can do. The tungsten target plate effectively represents an additional particle sink for a few *ms* which can be defined as required *refill-time*. According to EDGE2D-EIRENE studies of the ELM-cycle [59] of a moderate additional heated H-mode plasma in the JET-ILW (#83621-83791, $B_t = 2.0$ T, $I_P = 2.0$ MA, $P_{aux} = 12$ MW, $\Delta W_{ELM} = 160$ kJ, $\Delta T_{ELM} = 150$ K and further details in [15]), a transient particle sink after an ELM-crash can be the cause for a delayed recovery of the pedestal density and a longer lasting ELM of up to 8 ms though the time scale of the MHD ELM-crash remains almost identical between JET-C and JET-ILW as described in [58]. However, it should be noted that the physical particle reservoir to be desorbed is limited whereas the ion flux to the target can increase e.g. with the plasma current and auxiliary power in H-mode discharges. Therefore, the transient phase with $R < 1$ at the target plate, effectively the refill-time, gets shorter with larger impinging ion flux and plasma current. Indeed such a behaviour has been seen in H-mode plasmas with plasma current increase [58]. Such an effect has not been observed for comparable moderate heated deuterium plasmas in JET-C which is likely caused by the large reservoir of fuel in co-deposits compensating quasi instantaneously the outgassing. Contrary, it can explain the different ELM-behaviour in helium in JET-C where no fuel reservoir exists in carbon PFCs.

5. Impurity content, radiation pattern and seeding

5.1. Impact of the impurity content on the plasma-edge behaviour

The exchange of carbon ($Z = 6$) by beryllium ($Z = 4$) and the reduction of the primary impurity source is reflected in the impurity concentration and the effective charge of the plasma (Z_{eff}). In JET-C, the line-averaged Z_{eff} deduced from Bremsstrahlung amounts 2.0 in the divertor phase with an averaged carbon concentration of about 3.0% in the plasma; variations depend on the plasma conditions [60]. With JET-ILW Z_{eff} shows typical values of 1.2 in deuterium fuelled H-mode plasmas and the averaged impurity composition can be described by a beryllium concentration of about $c_{Be} \simeq 1.1\%$ and a residual carbon contribution of about $c_C \simeq 0.1\%$ taken from spectroscopy. Fig. 9a shows typical Z_{eff}-profiles from charge-exchange recombination spectroscopy (CXRS) for a set of high triangularity plasmas in H-mode [21] at same current and magnetic field: Z_{eff} is for the pure deuterium JET-ILW plasma about $Z_{eff} = 1.1$ and the profile is absolute flat. This is in contrast to the carbon-dominated Z_{eff}-profile in JET-C which is about an order of magnitude higher and slightly hollow. Moderate nitrogen seeding recovers the Z_{eff}-profile shape and magnitude which is likely related to the comparable radiation capabilities of nitrogen and carbon. In ASDEX Upgrade Z_{eff}, amounts typically to 1.4 in discharges shortly after a boronisation and 1.7 in discharges long after a boronisation [61], thus, Z_{eff} is even without impurity seeding close to values obtained in JET-ILW with nitrogen seeding. Responsible are residual levels of low-Z impurities (C, O and F) in the ASDEX Upgrade plasma. The impact of boron on the plasma purity in ASDEX Upgrade can be compared to beryllium in JET-ILW with the difference that beryllium is acting permanently and boron only for a short period after a boronisation.

However, not only the Z_{eff}-profile recovers with seeding of nitrogen, also a number of plasma edge, respectively, pedestal properties are restored in comparison with changes observed in bare JET-ILW and JET-C discharges: (a) In unseeded plasmas, a reduction of the threshold power for the L-H transition in the low density branch was observed with the JET-ILW [62]. Nitrogen seeding inducing $Z_{eff} \simeq 2.0$ increases the L-H power threshold and restores almost the behaviour observed in JET-C [63]. (b) The loss of confinement in high triangularity discharges with deuterium fuelling of about 30% of the H-factor in the JET-ILW in comparison with JET-C reference discharges was reported before [20]. This loss in confinement has primarily been correlated to a reduction of the pedestal temperature (Fig. 9b) and partial recovery was observed with nitrogen seeding [64] and with increase of normalised plasma pressure β_N [20]. Indeed in the set of available discharges a correlation between the averaged Z_{eff} and the pedestal temperature was observed (Fig. 9b). Though in both cases a correlation with Z_{eff} is observed, the physics mechanisms and to which degree the impurity content and/or the impurity profile is responsible for the recovery is not known and subject of current intensive studies. However, similar correlations have been observed in ASDEX Upgrade with the installation of the all-W first wall and the usage of nitrogen seeding [7].

5.2. Divertor characterisation and density limit

A direct consequence of the practical absence of carbon is the loss of significant impurity-induced radiation cooling in the divertor plasma, which leads to an increase of the local T_e as well as impact energies of ions impinging on the target plate. This is caused by (a) the much lower cooling potential of beryllium in contrast to carbon under typical divertor temperatures of $T_e \simeq 30eV$ [65], and (b) the fact that also less beryllium (JET-ILW) as carbon (JET-C) is present in the divertor due to the lower primary source and the change of the migration pattern discussed before. Moreover, carbon in the carbon divertor of JET-C performed multiple

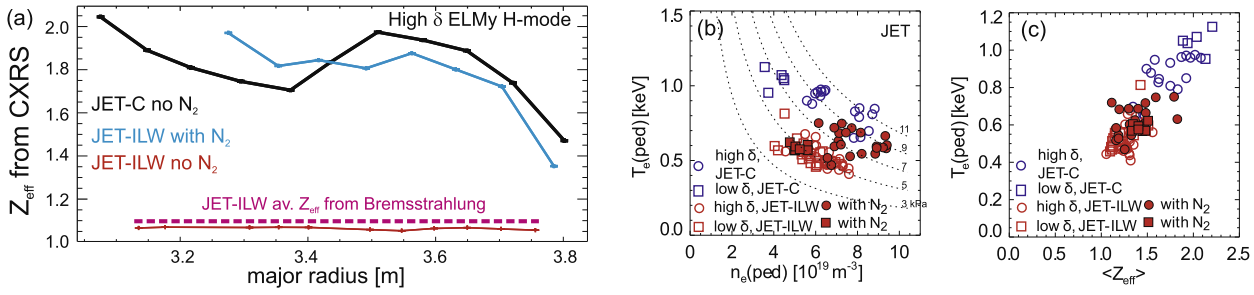

Fig. 9. (a) Radial profiles of Z_{eff} calculated from charge-exchange recombination spectroscopy for three conditions: deuterium fuelled JET-C, JET-ILW and N-seeded JET-ILW discharge. (b) Variation of the T_e^{ped} as function of n_e^{ped} and Z_{eff} for the three conditions and two plasma triangularities (high $\delta = 0.4$ and low $\delta = 0.2$) [20].

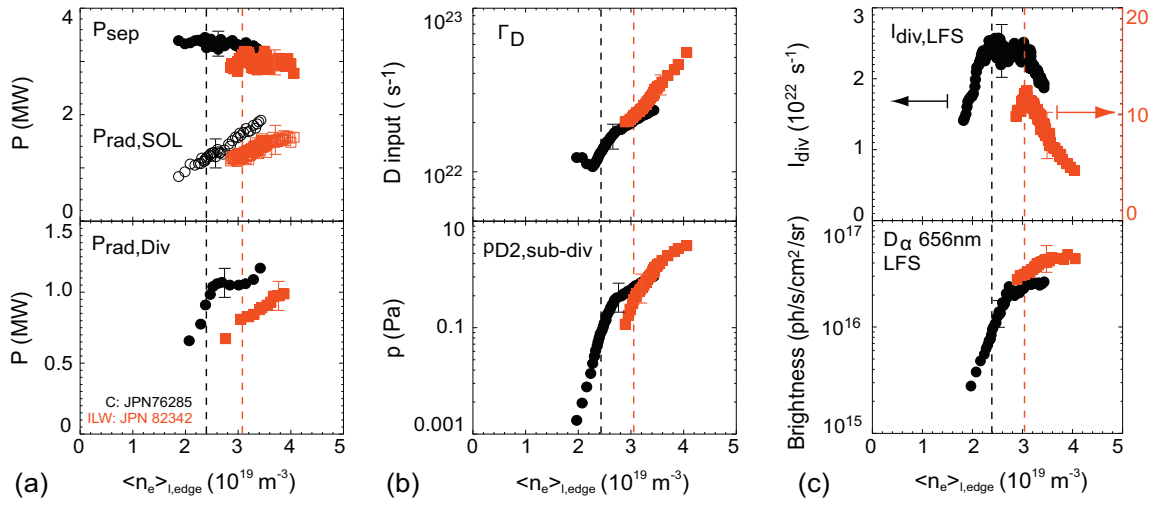

Fig. 10. Pair of comparable JET-ILW and JET-C L-mode density-ramp discharges: (a) radiated power, (b) deuterium throughput and divertor pressure, and (c) ion flux to and recycling flux at the outer-target plate. Complete ion-flux roll over and increase of the density limit with the JET-ILW.

erosion/deposition steps (≃10) before reaching the inaccessible pump-duct area [3] which enhances effectively the radiation capability of a single carbon by the same factor. In contrast, the incoming beryllium from the main chamber performs in the tungsten divertor only about two steps, caused by re-erosion owing to physical sputtering or reflection, before it sticks to the target material. The migration pattern and the chemical sputtering of carbon in the case of JET-C had vital impact on the divertor and SOL conditions whereas the (unseeded) JET-ILW case reveals almost the bare deuterium plasma. A series of experiments with density ramp-up discharges in different magnetic configurations have been applied to verify the T_e increase, the loss of divertor radiation, and to characterise the divertor plasma in the JET-ILW [66]. These purely deuterium fuelled experiments confirmed indeed a moderate increase of T_e in the W divertor in comparison with JET-C reference cases. The increase was moderate due to the fact that in the JET-C reference case in L-mode, impurity radiation contributed only about 20–30% of the total radiation (Fig. 10a); the vast amount was determined by deuterium radiation (Fig. 10b). However, the difference in residual impurity radiation has vital impact on the accessibility of the completely detached and recombining divertor regime as well as on the density limit (Fig. 10c).

Complete divertor detachment has been achieved in both legs providing even a window for stable MARFE operation with full recombining divertor, thus, full detachment and radiation at the *x*-point region [67]. Moreover, the density limit is increased by 20–30% revealing that in JET-C the limit was determined in-fact by a radiation limit caused by carbon before the empirical Greenwald density limit n_{GW} was achieved. The density limit in JET-C and JET-ILW takes still place at the same total radiation, but as beryllium is not significantly contributing to the divertor radiation, more deuterium is required to compensate and radiates in the divertor. As the deuterium gas throughput is further increased, the maximum achievable density overcomes finally the empirical Greenwald limit with $n_{ILW}/n_{GW} = 1.05$ before a disruption occurs. Minor variations in the absolute numbers depend on the actual magnetic configuration. The available data set of well diagnosed discharges in different magnetic configurations is applied to benchmark the plasma boundary code SOLPS [68], also used for ITER predictions [69], and EDGED2D-EIRENE [70] reproducing the general behaviour [71], but still cannot match the exact in-out asymmetry of the radiation pattern in the divertor. Nevertheless, the JET-ILW experiments widen the operational window with semi- or even completely-detached divertor operation with respect to earlier studies in JET-C.

6. Summary and conlcusion

The JET ITER-Like Wall experiment provides for the first time an insight in the coupling between tokamak-plasma operation and plasma-surface interaction in the Be/W material environment and acts as test-bed to verify physics models and modelling tools for ITER. The cross-correlation of the main plasma-surface interaction processes employing a beryllium wall and a tungsten divertor: (a) material erosion and migration, (b) fuel recycling and retention, (c) impurity concentration and radiation, were established and the newly gained physics understanding compared with earlier observations and physics interpretation in JET with all-carbon first wall as well as in other metallic tokamaks. The inter-connection of plasma-surface interaction with plasma-edge physics such as pedestal or divertor properties revealed that both interpretation of previously obtained JET-C results and predictions to ITER need to be revisited. The impact of the first wall material on the plasma performance as well as the prominent role of chemical erosion of carbon were underestimated: carbon in the plasma, eroded from the plasma-facing components, masked partially the plasma behaviour and properties which were attributed solely to the deuterium plasma.

(a) The change in the material migration with the JET-ILW in divertor configuration is one key result as it impacts directly or indirectly on the majority of PSI processes mentioned above and corrects partially the migration pattern predictions made in [4] for Be/W PFCs: the primary beryllium source in JET-ILW is lower than the carbon source in JET-C. As consequence of the lower initial source is the inner divertor not covered by beryllium, but intact tungsten surfaces exist, and the absence of beryllium sputtering at low impact energies inhibits the cycle of multiple erosion/deposition within the divertor. Instead beryllium remains deposited at the positions where it lands or performs one more step by reflection/physical sputtering above the energetic threshold. However, it should be noted that the JET-ILW migration pattern might not yet be in full equilibrium due to limited operational time and could therefore represent an intermediate state with respect to long-pulse operation.

(b) The second key result is the reduction in long-term fuel retention with the JET-ILW confirmed by gas balances, post-mor-

tem analysis and WallDYN modelling. The remaining long-term retention is caused by implantation and co-deposition with beryllium and residual impurities. Short-term retention gained relative importance with respect to the low level of long-term retention and impacts on the recycling properties of both beryllium and tungsten and local plasma conditions. Predictions to ITER with WallDYN indicate more than 3000 DT-discharges before the fuel-inventory limit is reached, thus, the need to apply very often fuel removal techniques is no longer given.

(c) The low effective charge of the plasma ($Z_{eff} = 1.2$) and the low radiation capability of beryllium reveals the bare deuterium plasma physics in the tokamak. Moderate impurity seeding with nitrogen, reaching $Z_{eff} = 1.6$ close to the ITER-reference value, restores in particular the confinement and the L-H threshold behaviour. ITER-compatible divertor conditions with stable semi-detachment have been achieved widening the operational window before density limit disruptions occur. The reduction of the impurity concentration in the plasma edge and the primary erosion source is similar to the situation observed in helium plasmas in JET-C. In both cases, the JET-ILW case with deuterium and the JET-C case with helium plasma, the fundamental process of chemical erosion at low impact energies is absent and can explain the drop in the impurity content which is then reflected in the corresponding values of Z_{eff} in the plasma core: $Z_{eff} = 1.2$ in JET-ILW deuterium plasmas, $Z_{eff} = 2.5$ in JET-C helium plasmas, and $Z_{eff} = 2.0$ in JET-C deuterium plasmas.

Overall JET demonstrated successful plasma operation in the Be/W material combination and confirms its advantageous behaviour with respect to material migration and fuel retention and gives strong support to the ITER material selection. Moreover, the recovery of the pedestal with changes in the recycling behaviour and the effective plasma charge with nitrogen indicates that plasma properties obtained in JET-C can be partially recovered at ITER-relevant effective plasma charge, but still using the benefit of the metallic wall with respect to the majority of plasma-interaction processes.

References

[1] A. Loarte et al., Nucl. Fus. 47 (2007) S203.
[2] G. Saibene et al., Plasma Phys. Contr. Fus. 44 (2002) 1769.
[3] G.F. Matthews et al., J. Nucl. Mater. 337–339 (2005) 1.
[4] J. Roth et al., J. Nucl. Mater. 390–391 (2009) 1.
[5] V. Arunasalam et al., Recent Results from the PLT tokamak, in: Proc. 8th Conf. EPS, Prague, vol. 2, 1977, pp. 17–28.
[6] B. Lipschultz et al., J. Nucl. Mater. 363 (2007) 1110.
[7] R. Neu et al., J. Nucl. Mater. 438 (2013) S34.
[8] A. Pospieszczyk et al., J. Nucl. Mater. 290–293 (2001) 947.
[9] R.A. Pitts et al., 55th APS Meeting (2014), Denver, CO, USA, paper WE1.00001.
[10] G. de Temmerman et al., Nucl. Fus. 48 (2008) 075008.
[11] R. Dux et al., J. Nucl. Mater. 390–391 (2009) 858.
[12] V. Philipps et al., Fus. Eng. Des. 85 (2010) 1581–1586.
[13] G.F. Matthews et al., J. Nucl. Mater. 438 (2013) S2.
[14] S. Brezinsek et al., J. Nucl. Mater. 415 (2011) S936.
[15] S. Brezinsek et al., Nucl. Fus. 53 (2013) 083023.
[16] E. Joffrin et al., Nucl. Fus. 54 (2014) 013011.
[17] S. Brezinsek et al., J. Nucl. Mater. 438 (2013) S303.
[18] A. Widdowson et al., Phys. Scr. T159 (2014) 014010.
[19] J.W. Coenen et al., J. Nucl. Mater. 463 (2015) 78–84.
[20] M.N.A. Beurskens et al., Plasma Phys. Control. Fus. 55 (2013) 124043.
[21] C. Giroud et al., Plasma Phys. Control. Fus. 57 (2015) 14039.
[22] G.F. Matthews et al., Phys. Scr. T145 (2011) 014001.
[23] I. Nunes et al., Fus. Eng. Des. 82 (2007) 1846.
[24] V. Riccardo et al., Phys. Scr. T38 (2009) 014033.
[25] G. Arnoux et al., Phys. Scr. T159 (2014) 014009.
[26] J. Horacek et al., J. Nucl. Mater. 463 (2015) 385–388.
[27] D. Douai et al., J. Nucl. Mater. 438 (2013) S1172.
[28] P. de Vries et al., Nucl. Fus. 53 (2013) 053003.
[29] W. Eckstein et al., Report IPP 9/132, 2002.
[30] S. Brezinsek et al., Nucl. Fusion 54 (2014) 103001.
[31] D. Borodin et al., J. Nucl. Mater. 438 (2013) S267.
[32] D. Borodin et al., Phys. Scr. T145 (2011) 014008.
[33] C. Björkas et al., New J. Phys. 11 (2009) 123017.
[34] R.P. Doerner et al., J. Nucl. Mater. 438 (2013) S272.
[35] A. Baron-Wiechec et al., this conference.
[36] K. Krieger et al., J. Nucl. Mater. 438 (2013) S262.
[37] R.A. Pitts et al., Plasma Phys. Control. Fus. 47 (2005) B303.
[38] S. Krat et al., J. Nucl. Mater. 456 (2015) 106.
[39] M. Mayer et al., J. Nucl. Mater. 438 (2013) S780.
[40] A. Kirschner et al., J. Nucl. Mater. 463 (2015) 116–122.
[41] H.G. Esser et al., this conference.
[42] K. Heinola et al., this conference.
[43] P. Petersson et al., J. Nucl. Mater. 463 (2015) 814–817.
[44] D. Ivanova et al., Phys. Scr. T159 (2014) 014011.
[45] G. van Rooij et al., J. Nucl. Mater. 438 (2013) S42.
[46] S. Brezinsek et al., Phys. Scr. T145 (2011) 014016.
[47] T. Pütterich et al., Plasma Phys. Control. Fus. 55 (2013) 124036.
[48] T. Loarer et al., J. Nucl. Mater. 390–391 (2009) 20.
[49] T. Loarer et al., J. Nucl. Mater. 438 (2013) S108.
[50] V. Philipps et al., J. Nucl. Mater. 438 (2013) S1067.
[51] V. Philipps et al., J. Vac. Sci. Technol. 11 (1993) 437.
[52] T. Loarer et al., J. Nucl. Mater. 463 (2015) 1117–1121.
[53] T. Wauters et al., J. Nucl. Mater. 463 (2015) 1104–1108.
[54] S. Romanelli-Grünhagen et al., Phys. Scr. T159 (2014) 014068.
[55] R.P. Doerner et al., Nucl. Fus. 49 (2009) 035002.
[56] K. Schmid et al., J. Nucl. Mater. 415 (2011) S284.
[57] K. Schmid et al., J. Nucl. Mater. 463 (2015) 66–72.
[58] B. Sieglin et al., Plasma Phys. Control. Fus. 55 (2013) 124039.
[59] D. Harting et al., J. Nucl. Mater. 463 (2015) 493–497.
[60] J.W. Coenen et al., Nucl. Fus. 53 (2013) 073043.
[61] A. Kallenbach et al., Nucl. Fus. 49 (2009) 045007.
[62] C.F. Maggi et al., Nucl. Fus. 54 (2014) 023007.
[63] C.F. Maggi et al., presented at the EPS 2014.
[64] C. Giroud et al., Nucl. Fus. 53 (2013) 113025.
[65] A. Kallenbach et al., J. Nucl. Mater. 415 (2011) S19.
[66] M. Groth et al., Nucl. Fus. 53 (2013) 083032.
[67] A. Huber et al., J. Nucl. Mater. 438 (2013) S139.
[68] L. Aho-Mantila et al., J. Nucl. Mater. 463 (2015) 546–550.
[69] A. Kukushkin et al., Fus. Eng. Des. 86 (2011) 2865.
[70] S. Wiesen et al., EDGE2D-EIRENE coupling, JET-ITC project report, 2006, <http://www.eirene.de>.
[71] C. Guillemaut et al., Nucl. Fusion 54 (2014) 093012.